A fibre optic fluorescence quenching oxygen partial pressure sensor using PtOEP

JOHN J. DAVENPORT[1,*], MICHELLE HICKEY[1], JUSTIN P. PHILLIPS[1], PANAYIOTIS A. KYRIACOU[1]

[1]*Research Centre for Biomedical Engineering (RCBE), City University London, UK*
**Corresponding author: john.davenport.1@city.ac.uk*

The development and bench testing of a fibre optic oxygen sensor is described. The sensor is designed for measurement of tissue oxygen levels in the mucosa of the digestive tract. The materials and construction are optimised for insertion through the mouth for measurement in the lower oesophagus. An oxygen sensitive fluorescence quenching film was applied as a solution of platinum octaethylporphyrin (PtOEP) poly(ethyl methacrylate) (PEMA) and dichloromethane and dip coated onto the distal tip of the fibre. The sensor was tested by comparing relative fluorescence when immersed in liquid water at 37 °C, at a range of partial pressures (0 – 101 kPa). Maximum relative fluorescence at most oxygen concentrations was seen when the PtOEP concentration was 0.1 g.L-1, four layers of coating solution were applied and a fibre core radius of 600 µm was selected, giving a Sterm-Volmer constant of 0.129 kPa-1. The performance of the sensor is suitable for many in-vivo applications particularly mucosal measurements. It has sufficient sensitivity, is sterilisable and is sufficiently flexible and robust for insertion via the mouth without damage to the probe or risk of harm to the patient.

1. INTRODUCTION

A. Oxygen partial pressure sensing

Aerobic cellular respiration depends on an adequate supply of oxygen and nutrients to the mitochondria; indeed interruption of the oxygen cascade from the environment to the subcellular environment can lead to hypoxia [1]. Efficient oxygen delivery depends on the co-ordinated interplay between the respiratory and circulatory systems [2, 3]. Measurement of local tissue oxygen partial pressure (oxygen tension) can therefore give vital information regarding the availability of oxygen at the tissue level the balance between local oxygen delivery and consumption at a given time.

Currently most sensors used for both in-vitro and in-vivo studies are based on the Clark electrode, which consists of a platinum anode and a silver cathode immersed in a silver chloride electrolyte solution [4]. The electrode surface is covered by a semi-permeable membrane, which allows oxygen molecules to pass through into the electrolyte solution where they are reduced at the cathode. An operational bias potential difference of approximately 0.65 V is applied across the electrodes. The resulting current flowing through the electrolyte solution is proportional to the partial pressure of oxygen diffusing to the reactive surface of the cathode. Clark electrodes are utilised in blood gas analysers and in cell biology for continuous in-vitro oxygen partial pressure (pO_2) measurement. Several companies have developed in vivo Clark electrodes for intravascular use or for implantation into tissue, most notably the brain, to monitor cerebral oxygenation following severe head trauma.

Clark electrode-based sensors have some limitations. Firstly, after introduction of the catheter there is a minimum 'settling-in' time, during which measurements are unstable. This is typically approximately two hours, but is sometimes much longer, probably due to micro-haemorrhages or possibly due to local vasoconstriction. In an animal study, small micro-haemorrhages were observed around a catheter tip placed in brain tissue, causing falsely low pO_2 readings [5]. Also, the overall accuracy of pO_2 sensors is sometimes doubted. One study showed pO_2 values of 0.93 ± 0.19 kPa in zero oxygen solution, suggesting that pO_2 values may be overestimated when they are at critically low levels [6].

Fluorescent quenching fibre optic sensors show promising potential for in-vitro pO_2 measurements and have been the focus of many recent studies [7, 8, 9]. Such sensors can be made small with fibre optic diameters typically between 200 and 1,000 µm, allowing them to be inserted into patients with minimum invasiveness or discomfort. Once inserted they can be used for accurate and continuous monitoring without the need for a prolonged settling-in period.

Fluorescence detection of oxygen combined with optical fibres presents unique opportunities for use as small size optical sensors and has been demonstrated by a number of groups [7, 8, 10, 11]. Chen et al. [7]

developed a cylindrical-core fibre optic sensor using platinum octaethylporphyrin; abbreviation: PtOEP, chemical formula: $Pt(NC_9H_{11})_4$ as a fluorophore. PtOEP was immobilised within a thin polymer film coated onto an optical fibre. When energised by light from a blue (450 nm) LED, the PtOEP on the sides and the tip of the fibre would fluoresce red (645 nm). The presence of oxygen molecules had the effect of quenching the fluorescent reaction, decreasing the intensity of the red fluorescence. By measuring the intensity of the red light, the partial pressure of oxygen could be found.

At least two commercial fibre optic pO_2 sensors existed at the time of writing, manufactured by Oxford Optronix [12, 13, 14] and Ocean Optics [15]. The former uses optical fibres with an external diameter between 250 µm and 650 µm [14] and the latter uses fibres with core diameters between 300 µm and 600 µm [16, 17] . Both coated the tips of the optical fibre in oxygen sensitive fluorescent materials developed in house. Chen et al. [18] developed a sensor using PtOEP coated onto an optical fibre with a tapered tip, demonstrating very rapid measurement times of 20 ms. Jiang et al. [19] developed a sensor using plastic optical fibres within a catheter tube for measuring pO_2 in the artieral blood of rabits.

B. Research aim

The primary aim of this work is to provide a new method of monitoring tissue gas partial pressures in the mucosa of the gastrointestinal tract by developing a combined pO_2 and pCO_2 sensor, the latter being developed in parallel to the pO_2 sensor at City University London. The wall of the gut is at risk of compromised blood flow leading to ischaemia in intensive care patients, often contributing to the onset of sepsis, septic shock and Multiple Organ Dysfunction Syndrome (MODS) [20, 21]. The lower oesophagus has been proposed as a suitable monitoring site for this application as it is readily accessible and is perfused by the gastrointestinal circulation [22]; therefore, any complications in the gastrointestinal tract should be detectable from the lower oesophagus. It has been proposed that an oesophageal sensor would allow for continuous and rapid detection of significant changes in gas partial pressures in the oesophageal mucosa from which deficiencies in gut perfusion could be inferred, enabling earlier and more successful intervention and aggressive restoration of mucosal blood flow [23].

By building on the work of Chen et al., a fibre optic sensor was developed and optimised specifically for use as an oesophageal oxygen sensor. This work differs from Chen et al. in its specific intended application where the previous work had been more general. Additionally this work used more standard multi-mode fibres with the fluorescent coating interacting with light from a central core on tip as the sides of the fibre were expected to be un-available if mounted inside an oesophageal probe. Optimisation for this specific function was carried out by considering the concentration of PtOEP in the coating mixture, number of coating layers on the optical fibre, and the core diameter of the optical fibre. Sensors were tested in liquid at 37 °C to ascertain their performance characteristics over a range of oxygen concentrations.

C. Measurement principle

Fluorescence occurs when a molecule, referred to as a fluorophore, is excited by light of one wavelength and then emits light of another, lower wavelength. This occurs when a photon is absorbed by the fluorophore, transferring energy and exciting an electron to a higher energy state. The fluorophore can then decay to a lower energy state and emit another photon.

Equation (1) shows the general case excitation of a fluorophore by a photon.

$$h\nu_{ex} + S_0 = S_1 \quad (1)$$

Here, S_0 is the ground (unexcited) state of the fluorophore and S_1 is the excited state of the fluorophore. h is Planck's constant (equal to 6.63×10^{-34} Js) and ν_{ex} is the frequency of the exciting photon. The general case of a fluorophore decaying and emitting a photon is shown in equation (2):

$$S_1 = S_0 + h\nu_{em} + E_{other} \quad (2)$$

where ν_{em} is the frequency of the fluorescent photon. E_{other} represents other forms of energy loss such as non-radiative dissipation as vibration (heat), or through additional photon emission. Values of E_{other} tend to depend on the specific electronic structure of the flurophore in question. In general, the energy of the emitting photon is smaller than that of the exciting photon, leading to a lower frequency and longer wavelength. Excitation and emission wavelengths are dependent on electron shell structure of the molecule and are specific to the fluorophore.

Fluorescence quenching occurs when excitation energy is transferred from the fluorophore to another chemical, referred to as a quencher. There are many mechanisms for this energy transfer including collision quenching, charge transfer or the formation of static complexes. Here we focus on collision quenching, one of the most common types and the mechanism responsible for oxygen quenching of PtOEP.

In collision quenching the fluorophore and the quencher interact and energy is transferred to the quencher. This prevents the fluorophore decaying photo-chemically and emitting its photon. By observing the decrease in fluorescence intensity, the concentration of the quencher can be ascertained. In the simplest case of a single collision-quenching path in a homogenous environment, the fluorescence intensity change caused by quenching is given by [7]:

$$I = \frac{I_0}{1+K_{sv}[O_2]} \quad (3)$$

where I is the fluorescence intensity in the presence of oxygen, I_0 is the intensity in its absence, K_{sv} is the Stern-Volmer quenching constant and $[O_2]$ is the oxygen concentration. K_{sv} is specific to the combination of fluorophore and quencher and is equal to the product of τ_0, the lifetime of the excited fluorophore and k, the bi-molecular rate.

The values of I_0 and K_{sv} depend on the intensity and coupling efficiency of the excitation light source, the quantity and concentration of the fluorophore, temperature of the environment and the specific efficiency of collisions between PtOEP and oxygen. The values of I_0 and K_{sv} can be found for a given device to allow oxygen concentration to be calculated.

2. MATERIALS AND METHODS

A. Sensor fabrication and setup

The PO_2 sensors developed in this study were made by dip coating a layer of oxygen sensitive material onto the distal tip of an optical fibre. A range of optical fibres were obtained for testing the variation of fibre diameter. A summary of their details and properties is given in Table 1. All fibres were obtained from Thorlabs Inc, Newton, US [24].

Table 1. Properties of the optical fibres used to test the effect of core diameter. Data from manufacturer's specification sheet [24].

Fibre	Core Diameter	Core material	Numerical aperture	Bend radius (momentary)
BFL48-400	400 µm	Silica	0.48	40 mm
BFL48-600	600 µm	Silica	0.48	60 mm
BFL48-1000	1,000 µm	Silica	0.48	100 mm

The tip was then placed in contact or submerged into a sample. The interaction between the sensing layer and oxygen in the sample allowed the oxygen partial pressure of the sample to be measured. Fig. 1 shows

a diagram of the distal tip of the sensor. The sensing layer contains fluorophore molecules (PtOEP) fixed in position by poly(ethyl methacrylate). Blue (460 nm) LED light was shown down the optical fibre to activate the fluorophore, which fluoresced red (550 nm) in the absence of oxygen. When oxygen was present, it quenched the fluorescent molecules, decreasing the intensity of the red light.

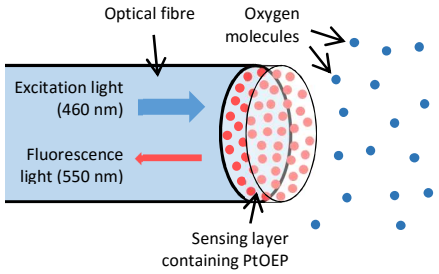

Fig. 1. Diagram of the distal tip of the PO2 optical fibre sensor. The sensing layer contains PtOEP molecules which fluoresce under 460 nm (blue) light, returning 550 nm (red) light. Oxygen molecules quench this fluorescence, allowing their concentration to be ascertained.

Three chemicals were used to create the coating solution: platinum octaethylporphyrin (PtOEP, $Pt(NC_9H_{11})_4$, CAS: 31248-39-2 [25]) as a fluorophore, poly(ethyl methacrylate) (PEMA, $[CH2C(CH3)(CO2C2H5)]_n$ CAS: 9003-42-3 [26]) as a fixer and dichloromethane (CH_2Cl_2 CAS: 75-09-2 [27]) as a solvent. All three were obtained from Sigma-Aldrich Corporation, St. Louis, USA.

PtOEP and PEMA powder was mixed with CH_2Cl_2 liquid in a glass vial. 100 mg PEMA was used to 2.0 ml CH_2Cl_2. The quantity of PtOEP was varied depending on the desired concentration, based on its molecular mass of 727.84 $g.mol^{-1}$ [25]. For each batch the vial was left to stand until the powders had completely dissolved.

The chemical coating was applied using a precision dip coater (precision dip coater, model - QPI-168, Qualtech Products Industry, Denver, USA) with a withdrawal rate range of 83 $nm.s^{-1}$ – 6.7 $mm.s^{-1}$ and a resolution of 17 $nm.s^{-1}$. It was set to lower the tip of the optical fibre into a vial of coating solution and then withdraw it at a set rate. Time was allowed between dips for the solvent to evaporate and the coatings to dry. Throughout the testing the immersion time was kept to 1s, the minimum setting of the dip coater, to minimise solvent damage to previous coatings.

Sensors were mechanically spliced to an optical fibre splitter (bifurcated borosilicate fibre, 600 µm diameter multi-mode core, BIFBORO-600-2 supplied by Ocean Optics) connected to an LED (460 nm, Wurth Elektronik, 151033BS03000, RS Components, UK) and a spectrometer (Ocean optics HR4000) [28]. Fig. 2 shows a diagram of the optical layout of the system.

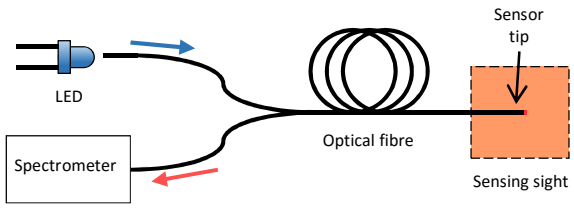

Fig. 2. Diagram of the optical layout of the sensor. The fibre splitter allows light from the LED to reach the sensing layer and excite the fluorophores, and fluorescent light to pass back to the spectrometer.

Blue light (460 nm) was introduced to the optical fibre using an LED, which then passed through the fibre splitter to the sensing layer. The sensing layer fluoresced red (550 nm), the intensity of which decreased in the presence of O_2. Some of the fluorescent light from the sensing layer returned along the optical fibre. The fibre splitter delivered this light to the spectrometer. By measuring the intensity of green light, the partial pressure of O_2 could be ascertained.

B. PO_2 Testing

The sensors were tested as shown in Fig. 3. The sensor was inserted into a conical flask containing liquid water in order to measure the pO_2. The partial pressure was controlled by bubbling gas at atmospheric pressure through the water and allowing at least 300 s for the dissolved gases to equilibrate. The gas input was made by combining flow from a 100 % nitrogen cylinder and a 100 % O_2 cylinder. Since the collision rate between oxygen molecules and the sensing layer is dependent on temperature, the conical flask containing the test sample was placed within a water bath kept at 37.0 ± 0.1 °C to mimic human body temperature.

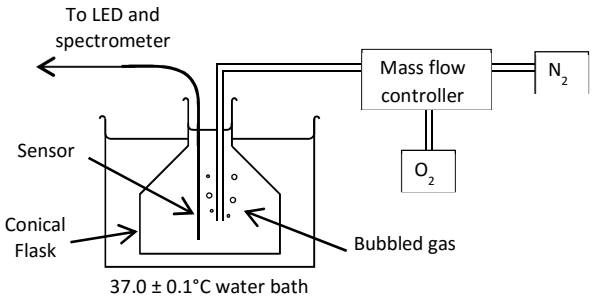

Fig. 3. Diagram of the setup used for testing the sensors. Oxygen concentration was controlled by bubbling gas through the water in the conical flask.

A total flow rate of 1000 $mL.min^{-1}$ was delivered from the two cylinders. Flow rates were measured and controlled using two FMA-A2406-SS-(N_2) mass flow controllers (Omega Engineering Ltd., Stamford, USA). The pO_2 was varied by altering the proportion of flow from the O_2 cylinder between 0 and 100 %. Details of the flow rates used are given in Table 2. Partial pressures were calculated based on atmospheric pressure of 101.3 kPa,

Table 2. Flow rates used of O_2 and N_2 to vary the percentage of O_2 measured by the sensor.

O_2 flow rate ($mL.min^{-1}$)	N_2 flow rate ($mL.min^{-1}$)	O_2 Percentage (%)	O_2 Partial pressure (kPa)
0	1,000	0 ±3	0 ±3
200	800	20 ±3	20 ±3
400	600	40 ±3	41 ±3
600	400	60 ±3	61 ±3
800	200	80 ±3	81 ±3
900	100	90 ±3	91 ±3
1,000	0	100 ±3	101±3

C. Form-factor and construction

1 General comments

The application of the sensor dictates certain design considerations and constraints, particularly regarding the dimensions and fabrication process of the sensor. Parameters were selected to maximise effective range of oxygen concentrations the sensors could reliably detect, as well as maximising sensitivity. It was also necessary to consider the physical constraints of the oesophagus when designing the sensor. The

oesophagus bends sharply between the mouth and the lower oesophagus. It was important to design the sensor to be able to take that bend without damage or endangering or injuring the patent. It is intended to encapsulate the sensor in a robust, biocompatible sheath before in-vivo studies but bend radius is an important consideration at this stage.

2 Fluorophore concentration

The effects of varying the concentration of PtOEP in the coating solution was investigated. Varying the concentration allowed the number of fluorophore molecules in the sensing layer to be controlled. Increasing the number of fluorophore molecules was expected to increase the intensity of fluorescent light emitted for a given oxygen concentration, thereby allowing smaller changes in oxygen concentration to be reliably detected. The effect of PtOEP concentration on fluorescent intensity and sensitivity was therefore investigated.

Table 3. Details of oxygen sensitive chemical mixes with varying fluorophore concentration.

Batch	PtOEP	PEMA	CH_2Cl_2	PtOEP Concentration
a	0.2 mg	100 mg	2.0 mL	0.1 $g.L^{-1}$
b	0.4 mg	100 mg	2.0 mL	0.2 $g.L^{-1}$
c	1.0 mg	100 mg	2.0 mL	0.5 $g.L^{-1}$
d	1.5 mg	100 mg	2.0 mL	0.75 $g.L^{-1}$

A series of solutions were mixed with variable PtOEP concentrations. The details are given in Table 3. A concentration of 0.1 $g.L^{-1}$, as used in batch a, was the lowest that could be accurately produced with the apparatus available as lower concentrations were below the precision of the measuring equipment that was used. A single coating was applied to the tip of 600 µm core optical fibres as described above. The resulting sensors were tested using the setup shown in Fig. 3.

3 Number of coating layers

The effects on the sensor response of the number of coating layers was also investigated. As with varying withdrawal rate, dipping the sensor into the coating solution multiple times was used to increase the coating thickness and thereby its sensitivity. Applying multiple layers allowed a greater thickness to be built up, although there was some potential for the solvent in the coating solution to remove some of the existing coating during the procedure.
A set of sensors were fabricated differing numbers of coating layers: one, two, three, four and five. Sensors used 600 µm cores and 0.1 $g.L^{-1}$ PtOEP solutions. A period of 30 minutes was allowed between layers to allow all previous coatings to dry. They were tested using the setup shown in Fig. 3.

4 Effect of fibre core diameter

The effects of the choice of optical fibre diameter were also investigated. A larger fibre diameter increased the surface area of the sensitive layer, thereby increasing the sensitivity of the sensor. However, it also increased the stiffness of the fibre and therefore increased the minimum bend radius, as was listed in Table 1.
Sensors used for this set of tests had a single coating and a fluorophore concentration of 0.1 $g.L^{-1}$. They were tested using the setup shown in Fig. 3.

3. RESULTS

1 Fluorophore concentration

Fig. 4 shows the sensor response to PO2 for a range of PtOEP concentrations in the sensing layer. All four fluorophore concentrations show a decrease in fluorescent intensity with increasing oxygen concentration consistent with the Stern-Volmer relationship Equation (3). The intensity of Sterm-Volmer signals can be seen to decrease with increasing PtOEP concentration with 0.1 $g.L^{-1}$ giving the strongest signal. As mentioned above, this was the lowest concentration available.

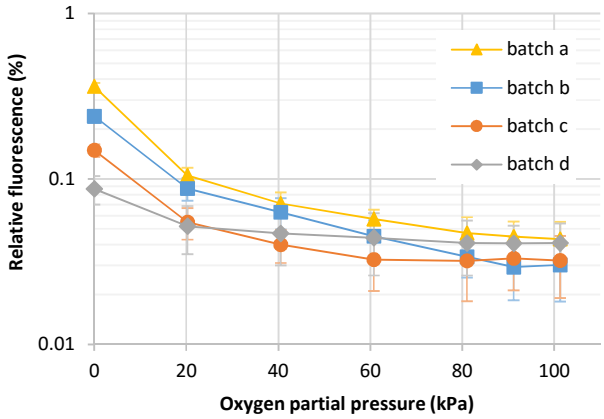

Fig. 4. Graph of sensor response to PO2 for a range of PtOEP concentrations in the sensing layer: Batch a, b, c and d containing PtOEP at 0.1 g.L-1, 0.2 g.L-1, 0.5 g.L-1 and 0.75 g.L-1.

2 Number of coating layers

Fig. 5 shows a graph of the sensor response to PO_2 for different numbers of coating layers. Signals generally follow a Stern-Volmer relationship with decreasing intensity with increasing oxygen concentration although an anonymously high result for two coats at 20 kPa. In general, the relative fluorescence increases slightly with increasing number of coats although the difference between three and four coats was minimal when compared to errors.

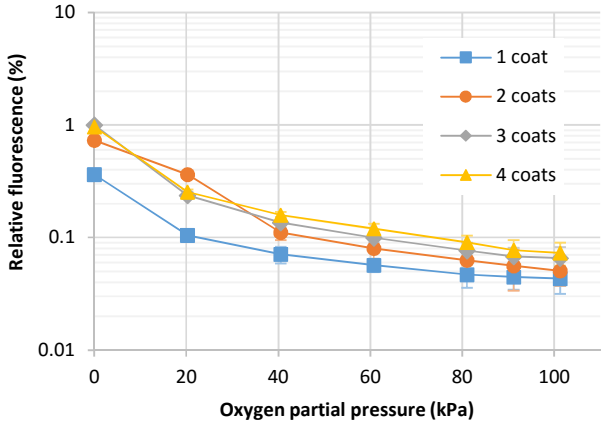

Fig. 5. Graph of sensor response to PO_2 using one to four coating layers.

3 Effect of fibre core diameter

Fig. 6 shows a graph of sensor response to PO2 for a range of fibre core diameters. As before, fluorescent intensity can be seen to decrease with

increasing oxygen concentration, consistent with the Stern-Volmer relationship. Strength of signal across oxygen concentrations is greater for greater core radius. This was believed to be predominantly due to the larger cross-section fluorescent material coating the tip of the fibre, although there may also have been improved coupling of light between the fibre and the coating.

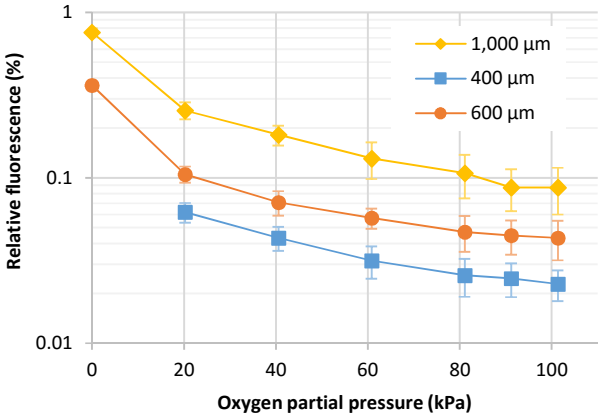

Fig. 6. Graph of sensor response to PO2 for a range of fibre core diameters: 200 µm, 400 µm, 600 µm and 1,000 µm.

The results show a clear correlation between sensitivity and core radius (and hence the active surface area of the sensor). To maximise the sensitivity, the largest available core radius should be selected, but this increases the minimum bend radius of the fibre. The tightest bend in the human oesophagus is at the connection to the mouth, with an approximate bend radius of about 70 mm [29]. The 600 µm fibre was therefore selected as its minimum bend radius of 60 mm does not exceed this. Table 4 gives the optimised parameters that were selected. Using Equation 3 and a least squares plot, the Sterm-Volmer constant for this setup was found to be 0.129 kPa^{-1}.

Table 4. Optimised parameters selected for the oxygen sensitive sensor.

Parameter	Selected value
Fluorophore concentration	0.1 g/l
Number of coating layers	Four
Fibre core diameter	600 µm

Fig. 7 shows the spectrometer data of the O_2 sensitive fluorescence peak for the parameters given in Table 4, for varying concentrations of O_2. The peak centres at 645 nm and follows a roughly Gaussian spread. It can clearly be seen that the intensity of the peak decreases with increased O_2, although signal from some of the higher concentration become difficult to distinguish above noise.

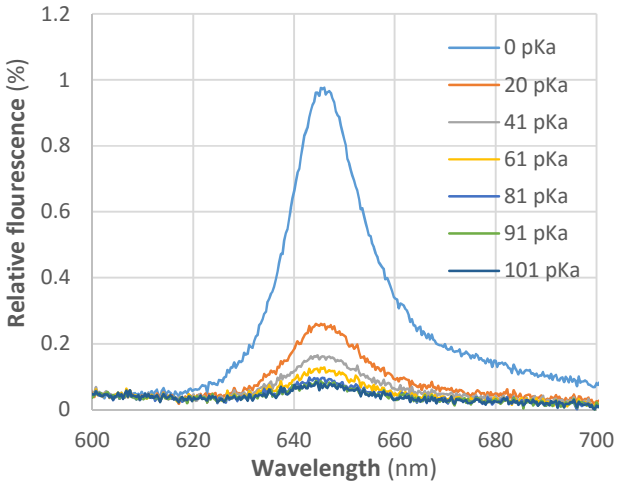

Fig. 7. Spectrometer data of the O_2 sensitive fluorescence peak for the parameters for a sensor fabricated using 0.1 g/l of PtOEP, a 600 µm fibre core diameter and four chemical coatings.

E. DISCUSSION AND CONCLUSION

The intention of this work was to select optimisation parameters for a fibre optic fluorescence quenching oxygen sensor for use in the lower oesophagus. Three parameters were investigated; fluorophore concentration, number of layers of the coating solution and fibre core radius. This allowed optimisation to a specific measurement site, maximising PO_2 sensitivity whilst maintaining a bend radius that could be readily inserted into the oesophagus.

The results clearly demonstrate sensitivity of fluorescent intensity to oxygen concentration as predicted by Equation (3). The aim was to maximise the intensity of measurable fluorescence to achieve sufficient sensitivity for clinically relevant oxygen measurement in the expected physiological range. The intensity of the fluorescence signal decreased with increasing concentration of the PtOEP fluorophore, with the highest intensity being at 0.1 $g.L^{-1}$. It was unclear why this was so, but a possible explanation was the higher concentrations of fluorescent molecules blocking excitation light from one another, or fluorescent light from returning to the sensor. Therefore, 0.1 $g.L^{-1}$ was selected as the optimal concentration. This was the lowest concentration tested and it was possible that a lower concentration would yield better results, but this was not possible without revising the fabrication process. Modifications to the fabrication process are currently being investigated.

The number of coating layers is the only purely discrete parameter, as only integer numbers of dips are possible. The strength of the signal was seen to increase slightly with increasing numbers of coatings, although little difference was seen between three and four layers. Four layers was therefore selected, although three would give similar results.

The optimized system compares favourably to current state of the art. For example the peak fluorescent intensity of this sensor was found to be approximately 30% higher than the Ocean Optics AL300-TM Oxygen Sensor Probe under similar conditions, potentially allowing for a greater signal to noise ratio and therefore increased sensitivity. It should be noted that the flexibillity is lower due to a greater optical fibre thickness. The optimisation of the techique worked well, showing an increase in measured intensity of more than ten times between the most and least optimised sensor parameters tested in this study.

This system has a number of advantages for use as an oesophageal probe. As discussed its bend radius is well suited to the curvature of the oesophagus and its sensitivity has been optimised within that

constraint. The optical fibre used was made from bio-compatible materials, making it suitable for use in the body. Alternatively the sensor could be contained within a flexible tube, which would protect the fibre from damage and ensure that if it were to break, parts would not come into contact with the patient.

The tip of the sensor may be coated in gas permeable silicone to prevent any damage to it during use. This would be expected to decrease the response time of the sensor as time would be required for oxygen to diffuse through the coating. In the intensive care unit, changes to be monitored tend to occur on the scale of minutes. Testing would be required to determine if response times could be found within this scale.

Sterilisation is an important consideration for sensors in vivo sensors. The optical fibres can be sterilised by most modern methods including autoclaving and ethylene oxide (EtO). The chemical coating on the tip of the sensor is not stable enough to withstand direct exposure to heat or EtO so would have to be either fabricated under sterile conditions or, more probably, sterilised using the EtO process after the application of a silicone coating.

To conclude, a fibre optic pO_2 sensor was fabricated based on the oxygen sensitive fluorescent chemical PtOEP. The sensor was optimised for use in the lower oesophagus. The sensor has a number of advantages including high sensitivity, electrical isolation, ease of sterilisation and sufficient flexibility to be inserted into the oesophagus without damage to the probe or risk of harm to the patient. Future work will include encapsulating the sensor in a protective, biocompatible sheath and carrying out in-vivo investigations in intensive care patients.

Acknowledgment.

This report is independent research funded by the National Institute for Health Research (Invention for Innovation (i4i) program, Development of a multi-parameter oesophageal sensor for the early detection of Multiple Organ Dysfunction Syndrome (MODS), II-LA-0313-20006). The views expressed in this publication are those of the author(s) and not necessarily those of the NHS, the National Institute for Health Research or the Department of Health.

References

[1] E. M. Nemoto, "Pathogenesis of cerebral ischemia-anoxia," *Critical Care Medicine,* vol. 6, pp. 203-14, 1978.

[2] R. Moradkhan and L. I. Sinoway, "Revisiting the Role of Oxygen Therapy in Cardiac Patients," *Journal of the American College of Cardiology,* vol. 56, no. 13, p. 1013–1016, 2010.

[3] A. Lumb, Nunn's Applied Respiratory Physiology, 7th edition, London: Churchill Livingstone, 2010.

[4] B. Middleton, J. P. Phillips, R. Thomas and S. Stacey, Physics in Anaesthesia, Oxford: Scion Books, 2012.

[5] W. A. VanDenBrink, I. K. Haitsma, C. J. Avezaat, A. B. Houtsmuller, J. M. Kros and A. I. Maas, "Brain parenchyma/pO2 catheter interface: a histopathological study in the rat," *Journal of Neurotrauma,* vol. 15, pp. 813-24, 1998.

[6] A. B. Valadka, S. P. Gopinath, C. F. Contant, M. Uzura and C. S. Robertson, "Relationship of brain tissue PO2 to outcome after severe head injury," *Critical Care Medicine,* vol. 26, pp. 1576-81, 1998.

[7] R. Chen, A. D. Farmery, A. Obeid and C. E. W. Hahn, "A Cylindrical-Core Fiber-Optic Oxygen Sensor Based on Fluorescence Quenching of a Platinum Complex Immobilized in a Polymer Matrix," *IEEE Sensors Journal,* vol. 12, no. 1, pp. 71-75, 2012.

[8] F. Formentia, R. Chen, H. McPeak, M. Matejovic, A. D. Farmerya and C. E. W. Hahn, "A fibre optic oxygen sensor that detects rapid PO2 changes under simulated conditions of cyclical atelectasis in vitro," *Respiratory Physiology & Neurobiology,* vol. 191, pp. 1-8, 2014.

[9] C. Chu, T. Sung and Y. Lo, "Enhanced optical oxygen sensing property based on Pt(II) complex and," *Sensors and Actuators B,* vol. 185, p. 287– 292, 2013.

[10] Y. Xiong, Z. Ye, J. Xu, Y. Zhu, C. Chen and Y. Guan, "An integrated micro-volume fiber-optic sensor for oxygen determination in exhaled breath based on iridium(III) complexes immobilized in fluorinated xerogels," *Analyst,* vol. 138, p. 1819–1827, 2013.

[11] X. Yang, L. Peng, L. Yuan, P. Teng, F. Tian, L. Li and S. Luo, "Oxygen gas optrode based on microstructured polymer optical fiber segment," *Optics Communications,* vol. 284, p. 3462–3466, 2011.

[12] T. Jarm, G. Sersa and D. Miklavcic, "Oxygenation and blood flow in tumors treated with hydralazine: Evaluation with a novel luminescence-based fiber-optic sensor," *Technology and Health Care,* vol. 10, p. 363–380, 2002.

[13] M. Urano, Y. Chen, J. Humm, J. A. Koutcher, P. Zanzonico and C. Ling, "Measurements of Tumor Tissue Oxygen Tension Using a Time-Resolved Luminescence-Based Optical OxyLite Probe: Comparison with a Paired Survival Assay," *Radiation Research,* vol. 158, pp. 167-173, 2002.

[14] Oxford Optronix Ltd., "Oxford Optronix, Sensors, Sensors for Oxygen Monitors," [Online]. Available: http://www.oxford-optronix.com/sensor12/sensor-for-Oxygen-Monitors.html. [Accessed 18th March 2016].

[15] F. Formenti, R. Chen, H. McPeak, M. Matejovic, A. D. Farmery and C. E. Hahn, "A fibre optic oxygen sensor that detects rapid PO2 changes under simulated conditions of cyclical atelectasis in vitro," *Respiratory Physiology & Neurobiology,* vol. 191, p. 1–8, 2014.

[16] Ocean Optics, "Ocean Optics, AL300-TM Oxygen Sensor Probe," [Online]. Available: http://oceanoptics.com/product/al300-tm-oxygen-sensor-probe/. [Accessed 19th March 2016].

[17] Ocean Optics , "Ocean Optics, PI600 Oxygen Sensor Probe," [Online]. Available: http://oceanoptics.com/product/pi600-oxygen-sensor-probe/. [Accessed 19th March 2016].

[18] R. Chen, F. Formenti, H. McPeak, A. N. Obeid, C. Hahn and A. Farmery, "Experimental investigation of the effect of polymer matrices on polymer fibre optic oxygen sensors and their time response characteristics using a vacuum testing chamber and a liquid flow apparatus," *Sensors and Actuators B,* vol. 222, p. 531–535, 2016.

[19] J. Jiang, L. Gao, W. Zhong, S. Meng, B. Yong, Y. Song, X. Wang and C. Bai, "Development of fiber optic fluorescence oxygen sensor in both in vitro and in vivo systems," *Respiratory Physiology & Neurobiology,* vol. 161, p. 160–166, 2008.

[20] S. M. Jakob, "Clinical review: Splachnicischaemia," *Critical Care,* vol. 6, pp. 306-312, 2002.

[21] C. L. Leaphart and J. J. Tepas, "The gut is a motor of organ system dysfunction," *Surgery,* vol. 141, pp. 563-569, 2007.

[22] F. H. Netter, The Netter Collection of Medical Illustrations: Digestive System: Upper Digestive Tract, 2nd ed, Volume 3 Part 1, Novartis Publications, 1997.

[23] A. Spanos, S. Jhanji, A. Smith, T. Harris and M. R. Pearse, "Early microvascular changes in sepsis, severe sepsis and septic shock," *Shock,* vol. 33, pp. 387-391, 2010.

[24] Thorlabs Inc., *Product Specification 0.48 NA Hard Polymer Clad Multimode Fiber,* Newton, USA: Thorlabs Inc., 2013.

[25] Sigma-Aldrich Coporation, *Product Specification, Platinum octaethylporphyrin - Dye content 98%,* St Louis, USA: Sigma-Aldrich Coporation, 2014.

[26] 2. Sigma-Aldrich Coporation, *Specification Sheet, Poly(ethyl methacrylate) – average Mw ~515,000 by GPC, powder,* St Louis, USA: Sigma-Aldrich Coporation, 2014.

[27] Sigma-Aldrich Coporation, *Product Specification, Dichloromethane – contains amylene as stabilizer, ACS reagent, ≥99.5%,* St Louis, USA: Sigma-Aldrich Coporation, 2014.

[28] Ocean Optics HR4000 Data Sheet, *Technical Data Sheet,* Ocean Optics, Dunedin, Florida, USA, 2011.

[29] E. N. Maroeb, "Overview of the Digestive System," in *Human Anatomy*, Menlo Park, USA, Benjamin/Cummings, 1997, p. 568.

[30] Omaga Engineering Limited, "FMA-A2100's, FMA-A2300's Massflow Meters FMA-A2200's, FMA-A2400's Massflow Controllers User's Guide," Omaga Engineering Limited, Stamford, USA, 2001.